View metadata, citation and similar papers at core.ac.uk

brought to you by CORE

provided by Edinburgh Research Explorer

THE UNIVERSITY of EDINBURGH

Edinburgh Research Explorer

Fibroblasts activation and abnormal extracellular matrix remodelling as common hallmarks in three cancer-prone genodermatoses

Citation for published version:
Chacón-Solano, E, León, C, Díaz, F, García-García, F, García, M, Escámez, MJ, Guerrero-Aspizua, S, Conti, CJ, Mencía, Á, Martínez-Santamaría, L, Llames, S, Pévida, M, Carbonell-Caballero, J, Puig-Butillé, JA, Maseda, R, Puig, S, de Lucas, R, Baselga, E, Larcher, F, Dopazo, J & Del Río, M 2019, 'Fibroblasts activation and abnormal extracellular matrix remodelling as common hallmarks in three cancer-prone genodermatoses', *British journal of dermatology*. https://doi.org/10.1111/bjd.17698

Digital Object Identifier (DOI):
10.1111/bjd.17698

Link:
Link to publication record in Edinburgh Research Explorer

Document Version:
Peer reviewed version

Published In:
British journal of dermatology

General rights
Copyright for the publications made accessible via the Edinburgh Research Explorer is retained by the author(s) and / or other copyright owners and it is a condition of accessing these publications that users recognise and abide by the legal requirements associated with these rights.

Take down policy
The University of Edinburgh has made every reasonable effort to ensure that Edinburgh Research Explorer content complies with UK legislation. If you believe that the public display of this file breaches copyright please contact openaccess@ed.ac.uk providing details, and we will remove access to the work immediately and investigate your claim.

OPEN ACCESS

Download date: 11. May. 2020

Accepted Article

PROFESSOR CLAUDIO J CONTI (Orcid ID : 0000-0003-4753-0722)

DR FERNANDO LARCHER LAGUZZI (Orcid ID : 0000-0002-6771-3561)

Article type : Original Article

Fibroblasts activation and abnormal extracellular matrix remodelling as common hallmarks in three cancer-prone genodermatoses

E. Chacón-Solano[1,2*], C. León[1,2,*], F. Díaz[1,2,*], F. García-García[3], M. García[1,2,4], M.J. Escámez[1,2,4], S. Guerrero-Aspizua[1,2,4], C.J. Conti[1,2], Á. Mencía[1,2], L. Martínez-Santamaría[1,2], S. Llames[2,4,5], M. Pévida[5], J. Carbonell-Caballero[6], J.A. Puig-Butillé[7], R. Maseda[8], S. Puig[7], R. de Lucas[8], E. Baselga[9], F. Larcher[1,2,4,&], J. Dopazo[10,11,12,&], M. del Río[1,2,4,&]

*These authors contributed equally

[&]Corresponding authors: Fernando Larcher, Joaquin Dopazo and Marcela Del Río emails: fernando.larcher@ciemat.es, joaquin.dopazo@juntadeandalucia.es, mrnechae@ing.uc3m.es

Affiliations:

[1]Department of Bioengineering, Universidad Carlos III de Madrid, Madrid, Spain.

[2]Regenerative Medicine and Tissue Engineering Group, Fundación Jiménez Díaz (IIS-FJD), Madrid, Spain.

[3]Bioinformatics and Biostatistics Unit, Centro de Investigación Príncipe Felipe (CIPF), Valencia, Spain.

[4]Epithelial Biomedicine Division, CIEMAT-CIBERER (U714), Madrid, Spain.

[5]Tissue Engineering Unit, Centro Comunitario Sangre y Tejidos (CCST), Oviedo, Spain.

[6]Department of Computational Genomics, Centro de Investigación Príncipe Felipe (CIPF), Valencia, Spain.

[7]Melanoma Unit, Hospital Clinic & IDIBAPS (Institut d'Investigacions Biomèdiques Agustí Pi i Sunyer), CIBERER (U726), Universitat de Barcelona, Barcelona, Spain.

[8]Department of pediatric dermatology, La Paz Hospital, Madrid, Spain.

Accepted Article

[9]Department of pediatric dermatology, Santa Creu I Sant Pau Hospital, Barcelona, Spain.

[10]Clinical Bioinformatics Area, Fundación Progreso y Salud, CDCA, Hospital Virgen del Rocío, Sevilla, Spain.

[11]Functional Genomics Node, INB-ELIXIR-es, FPS, Hospital Virgen del Rocío, Sevilla, Spain.

[12]Bioinformatics in Rare Diseases (BiER-U715), CIBERER, FPS, Hospital Virgen del Rocío, Sevilla, Spain.

Short title: Common expression signature in fibroblasts of cancer-prone genodermatoses

Funding sources

This study was supported by grants from Spanish Ministry of Economy and Competitiveness (SAF2013-43475R, SAF2017-88908-R and SAF2017-86810-R); from Instituto de Salud Carlos III and CIBERER, co-funded with European Regional Development Funds (ERDF) (PT13/0001/0007, PI14/00931, PI15/00716, PI15/00956, PT17/0009/0006 and PI17/01747); and from European Union (HEALTH-F2-2011-261392 and H2020-INFRADEV-1-2015-1 / ELIXIR-EXCELERATE-ref.676559). Additional funding comes from Comunidad de Madrid (AvanCell-CM S2017/BMD-3692); Catalan Government (AGAUR 2014_SGR_603); "Fundació La Marató de TV3, 201331-30"; CERCA Programme/Generalitat de Catalunya; and "Fundación Científica de la Asociación Española Contra el Cáncer", Spain.

Conflicts of interest

The authors state no conflict of interest.

What's already known?

- Recessive dystrophic epidermolysis bullosa (RDEB), Kindler syndrome (KS) and Xeroderma pigmentosum complementation group C (XPC) are three genodermatoses with high predisposition to cancer development.

Accepted Article

- Although their causal genetic mutations mainly affect epithelia, the dermal microenvironment likely contributes to the physiopathology of these disorders.

What does this study add?

- We disclose a large gene transcription overlapping profile between XPC, KS and RDEB fibroblasts that point towards an activated phenotype with high matrix-synthetic capacity.
- This common signature seems to be independent of the primary causal deficiency, but reflects an underlying derangement of the extracellular matrix via TGF-β signalling activation and oxidative state imbalance.

What is the translational message?

- This study broadens the current knowledge about the pathology of these diseases and highlights new targets and biomarkers for effective therapeutic intervention.
- It is suggested that high levels of circulating periostin could represent a potential biomarker in RDEB.

Summary

Background: Recessive dystrophic epidermolysis bullosa (RDEB), Kindler syndrome (KS) and Xeroderma pigmentosum C (XPC) are three cancer-prone genodermatoses whose causal genetic mutations cannot fully explain, on their own, the array of associated phenotypic manifestations. Recent evidence highlights the role of the stromal microenvironment in the pathology of these disorders.

Objectives: To investigate, by means of comparative gene expression analysis, the role played by dermal fibroblasts in the pathogenesis of RDEB, KS and XPC.

Methods: We conducted RNA-Seq analysis that included a thorough examination of the differentially expressed genes, a functional enrichment analysis and a description of affected signalling circuits. Transcriptomic data were validated at the protein level in cell cultures, serum samples and skin biopsies.

Accepted Article

Results: Inter-disease comparisons against control fibroblasts revealed a unifying signature of 186 differentially expressed genes and 4 signalling pathways in the three genodermatoses. Remarkably, some of the uncovered expression changes suggest a synthetic fibroblast phenotype characterized by the aberrant expression of extracellular matrix (ECM) proteins. Western blot and immunofluorescence *in situ* analysis validated the RNA-Seq data. In addition, enzyme-linked immunosorbent assay (ELISA) revealed increased circulating levels of periostin in RDEB patients.

Conclusions: Our results suggest that the different causal genetic defects converge into common changes in gene expression, possibly due to injury-sensitive events. These, in turn, trigger a cascade of reactions involving the abnormal ECM deposition and under-expression of antioxidant enzymes. The elucidated expression signature provides new potential biomarkers and common therapeutic targets in RDEB, XPC and KS.

Keywords: dystrophic epidermolysis bullosa, xeroderma pigmentosum, Kindler syndrome, RNA-Seq, TGF-ß, oxidative stress.

Introduction

The progress made in molecular genetics has greatly contributed to identify the primary causes of a large number of heritable skin diseases (1). However, these findings do not always explain by themselves the complex phenotypic manifestations observed in cancer-prone genodermatoses, such as Recessive dystrophic epidermolysis bullosa (RDEB), Kindler syndrome (KS) and Xeroderma pigmentosum complementation group C (XPC). RDEB is caused by loss-of-function mutations in the *COL7A1* gene, which encodes type VII collagen anchoring fibrils (C7), structures that connect the epidermal basement membrane to the dermal tissue. C7 deficiency causes loss of dermo-epidermal adhesion, resulting in blister formation, scarring and aggressive carcinoma development (2). KS results from recessive mutations in the *FERMT1* gene, encoding for kindlin-1. This protein mediates anchorage between the actin cytoskeleton and the extracellular matrix (ECM) via focal adhesions. KS is characterized clinically by early age acral skin blisters, photosensitivity, and high risk of mucocutaneous malignancies (3–5). XPC is characterized by mutations in the *XPC* gene, which cause a severe deficiency in the nucleotide excision repair pathway. XPC patients are

Accepted Article

highly sensitive to UV radiation and have a very high risk of developing skin tumours in sun-exposed areas, mostly basal and squamous cell carcinomas arising from epidermal keratinocytes, and malignant melanomas (6). XPC patients have also a high risk of developing tumours in internal organs not exposed to sunlight (7). Besides cancer susceptibility, other common clinical signs to the three genodermatoses are inflammation and premature skin aging (8–10). Although the specific primary and subsequent genetic alterations at the epidermal level are likely to be major drivers for carcinogenesis in these disorders, an altered stroma may be playing a facilitating role towards tumour development and malignant progression.

Robust data, gathered mainly from *omic* studies of patient cells and mouse models, underscore the role of an aberrant extracellular matrix deposition, leading to progressive fibrosis and cutaneous squamous-cell carcinoma (cSCC) in RDEB. This process appears to be mediated by the dermal fibroblasts, that acquire molecular changes similar to those present in tumour microenvironment (i.e. cancer associated fibroblasts; CAFs) (11). Less is known in this regard for KS and XPC, although marginal evidence indicates that fibroblasts may also be relevant in the disease pathogenesis (12–15). Here, we demonstrate through RNA-Seq analysis and expression validation of relevant genes that RDEB, XPC and KS fibroblasts allow to establish a common pro-fibrotic microenvironment that could favour disease progression and cancer.

Materials and methods

Sample collection and cell culture

All procedures were approved by the ethics committee of La Paz University Hospital (code HULP: PI-1602) and were conducted in accordance to the Declaration of Helsinki and subsequent revisions. Skin biopsies from unaffected areas of 7 healthy donors, 11 RDEB, 4 KS, and 4 XPC patients were obtained after written informed consent. Fibroblasts were isolated by mechanical and enzymatic digestion as previously described (16) and cultured in Dulbecco's Modified Eagle's Medium (Gibco, Invitrogen) supplemented with 10% foetal bovine serum (Gibco, Invitrogen) and 1% Antibiotic-Antimycotic (Life Technologies). The characteristics of the patients and controls can be seen in Table S1. All cells used were at early 3-7 passages.

Accepted Article

RNA extraction

Culture medium was changed 24h before harvesting the cells. Total RNA was isolated from confluent primary fibroblasts using RNeasy kit (Qiagen, Germany) according to the manufacturer's protocol recommendations. RNA concentration and quality was determined on a NanoDrop Spectrophotometer (Thermo Scientific) and integrity was verified with a Bioanalyzer 2100 (Agilent, USA). The RNA integrity number (RIN) was in all cases higher than 8,5. To minimize technical variability, RNA extracts from four technical replicates of each sample were mixed.

RNA-Seq data processing

cDNA libraries were generated for each sample using the TruSeq RNA Sample Preparation Kit (Illumina, CA) according to the recommended protocol. Ligation and library integrity was verified using an Agilent Bioanalyzer 2100. Sample libraries ligated with unique adapter sequences were multiplexed six to a lane and were sequenced by Edinburgh Genomics (Ashworth Laboratories, Scotland) using Illumina HiSeq HO v4 125 paired end sequencing. Quality control analysis on the resulting FASTQ files was performed using FastQC (Babraham Bioinformatics, UK). Reads were adapter trimmed using cutadapt version 1.3 with the parameters -q 30 -m 50 -a AGATCGGAAGAGC. Trimmed reads were aligned to Ensembl version 38.81 of the Homo sapiens genome with TopHat2 version 2.0.13 using default parameters (except "-r -70 -mate-std-dev 75" to specify insert sizes). The BAM files were sorted by name using Picard-tools (version 1.115) SortSam. Read counts were generated using HTSeq-count version 0.6.0 in unstranded mode, and Python version 2.7.3, with parameters -m union -i gene_id -t exon. Raw and processed data are stored at NCBI´s Gene Expression Omnibus, accession code GSE119501 (https://www.ncbi.nlm.nih.gov/geo/query/acc.cgi?acc=GSE119501).

RNA-Seq data were normalized using the Trimmed Mean of M values (TMM) (17). An adjustment for possible batch effects was performed using the R package ComBat (18). The transcripts that had an average expression per condition less than 1 count per million and a coefficient of variation per condition higher than 100% were filtered. Differential expression analysis was performed with the Bioconductor package edgeR (19). Conventional

multiple testing p-value correction procedure proposed by Benjamini–Hochberg was used to derive adjusted p-values (20). Enrichment analysis was carried out for the Gene Ontology (GO) terms using the Babelomics suite (21) as well as DAVID Bioinformatic resources (22).

Pathway activity analysis and protein-protein interaction

The signalling circuit activity analysis method (23), as implemented in the Hipathia R package (https://github.com/babelomics/hipathia), was applied to all disease vs healthy control comparisons. Under this modelling schema, signalling circuits are defined within KEGG pathways as the chain of proteins that connect a receptor protein to an effector protein that trigger specific cellular activities. The signal is propagated from the receptor protein along the proteins that compose the circuit by a recursive formula that takes into account the activity of both, activator and inhibitor proteins. Finally, the list of the common dysregulated genes in all disease versus controls comparisons was uploaded to STRING (24), a database that represents the known protein-protein interactions (PPI). The minimum required interaction score was set to >0.7 allowing only high confidence connections between nodes.

Western Blot analysis

Primary fibroblasts, serum-starved for 24h, were lysed with 25mM Tris-HCl (pH 7.4), 100mM NaCl, 1% Nonidet P-40, and protease inhibitor cocktail (Roche Diagnostic). The extracts were cleared for cellular debris by centrifugation at 16.000g for 15min at 4°C. Protein extracts were electrophoresed on SDS-PAGE 4-12%Bis-Tris gel and transferred onto nitrocellulose membranes. The membranes were blocked with 5% non-fat milk powder in 1X TBS for 1h at room temperature and incubated overnight with one of the following antibodies: anti-Tenascin-C (MAB2138; R&D Systems), anti-βIG-H3 (D31B8; Cell Signaling Technology), anti-ALDH1A1 (EP1933Y; Abcam), anti-Periostin (sc-398631), anti-Fibulin-1 (sc-25281), anti-TGase2 (sc-48387), and anti-GAPDH (sc-25778; Santa Cruz Biotechnology). Detection was performed using HRP-conjugated secondary antibodies and a chemiluminescent detection assay (SuperSignal West, Thermo Scientific). Three independent experiments were performed for each patient sample and controls.

Accepted Article

Accepted Article

Immunofluorescence analysis

Skin cryo-sections from 3 healthy donors, 2 RDEB and 2 KS patients were immunostained against tenascin-C (MAB2138) and periostin (sc-398631). Fluorescence quantification was measured using the ImageJ program. A Student's t-test was applied to compare the fluorescence intensity/area means of samples, using GraphPad Prism 5.04 software (La Jolla, CA).

Enzyme-linked immunosorbent assay (ELISA)

Serum samples from 16 RDEB and 10 healthy donors (Table S1b) were analysed using human periostin ELISA kit (EHPOSTN-PL; Thermo Scientific) according to the manufacturer's protocol. The absorbance was measured at 450nm and 550nm with a microtiter plate reader (TECAN Genios Pro, Austria). D'Agostino-Pearson omnibus test was applied to determine if the values have a normal distribution. Unpaired t-test with Welch's correction was done to determine the statistical significance between RDEB and controls (GraphPad Prism 5.04). Two independent experiments were performed for each patient sample and controls.

Results

Genodermatosis patients and mutations

Patients were screened for *COL7A1*, *XPC* and *FERMT1* specific mutations, according to the diagnosed disease (Table S1a). All RDEB patients were homozygous for a *COL7A1* recurrent mutation (c.6527insC), leading to a premature termination codon (PTC) (25). All the screened XPC patients carried a homozygous frameshift mutation (c.1643_1644delTG) in *XPC* gene, resulting in PTC. Finally, KS patients were the most heterogeneous group, with three different homozygous mutations in *FERMT1* gene. KS1 produce an altered splicing due to insertion of a new triplet (c.1371+4>G), KS2 is a missense variant (c.1198T>C) and KS3 has a frameshift mutation (c.676dupC).

Accepted Article

Identification of common expression signatures linked to fibroblast activation and ECM deposition

RNA-Seq counts were obtained for primary fibroblasts isolated from three healthy donors, nine RDEB, three KS, and three XPC patients. A total of 22.970 transcripts, identified by their Ensembl IDs, were obtained for each sample after quality data assessment and normalization (Table S2). The observed arrangement of the samples in the principal component analysis (PCA) discarded possible batch effect and organized the samples following the different disease groups. Notably, all genodermatosis samples are located in proximity within the plot, and distinctly separated from controls (Fig. 1a), pointing towards a similar transcription profile between the three genodermatoses.

In order to identify the dysregulated genes, differential expression analysis was carried out, contrasting each disease group (RDEB, KS or XPC) versus healthy controls (Table S3). The number of differentially expressed genes (FDR<0.05) in the different comparisons is detailed in Table 1. Venn diagram of the different comparisons revealed an intersection of 227 common dysregulated transcripts (containing 186 genes) in the three genodermatoses (Fig. 1b). Interestingly, all these transcripts (i.e. 129 upregulated and 98 downregulated) showed not only the same expression pattern (Fig. 1c), but also an impressive positive correlation between the fold changes (Fig. 1d). This suggests that the common expression profile may have a similar phenotypic impact on the three diseases.

Common expression patterns are best understood through the examination of enriched GO terms (26) and KEGG pathways (27). This approach provides an undirected method to highlight those biological mechanisms that could be potentially relevant to the diseases. The output of this enrichment analysis is a list of pathways and/or ontologies that involves a statistically significant number of dysregulated genes, associated to the same biological mechanism (Fig. 2, Table S4). Enriched GO terms for all the diseases point towards an abnormal relationship between the cell and its stroma. This suggests that the contribution of dermal fibroblasts to the disease lies in the altered response they exert on the surrounding microenvironment. The dysregulated genes were significantly associated with extracellular matrix and cell periphery (cellular component). Furthermore, glycosaminoglycan binding, sulfur compound binding and heparin binding - which point towards ECM components - are overrepresented (molecular function). Apart from these terms, an altered activity of transcription factors is also noticeable, presumably associated to the observed differences in

Accepted Article

gene transcription. KEGG pathway analysis identified common alterations in PI3K-Akt signalling, chemokine repertoire and two cancer-related pathways (highlighted terms in Table S4).

To gain a deeper insight into the altered mechanisms, we employed the web-tool *Hipathia* (http://hipathia.babelomics.org) to decompose KEGG pathways into signalling circuits, by transforming gene expression profiles into signal transduction activity profiles (23). We found 42 overlapping circuits in the three genodermatoses when comparing versus controls (Fig. S1a), with effectors associated to cell proliferation (*AREG*, *MAPK8*), TGF-β signalling (*PITX2*) and ECM-cell interactions (*PLAU*, *MAP3K4*) (highlighted terms in Table S5). A particular example of these circuits includes an activation of *BCL2* - as effector molecule of anti-apoptotic effect - initiated in multiple overexpressed nodes and propagated through the PI3K-Akt pathway (Fig. S1b).

To identify functional associations between the 186 differentially expressed genes STRING database (24) was used to generate PPI networks. The enrichment PPI p-value (0.00126) indicates that the commonly altered genes do not represent a randomly scattered set of proteins, but a meaningfully connected set of genes in accordance with its biological functions. Three major clusters (A, B and C) of proteins were detected (Fig. 3). Cluster A includes a group of proteins, mostly downregulated, involved in signalling pathways and signal transduction (e.g. *JAK3*, *PTK2B* and *PRKCQ*). Interestingly, this cluster also contains the angiotensin II receptor (*AGTR1*, upregulated), a target of recent anti-fibrotic therapy tested in RDEB (28), and the antioxidant enzyme extracellular superoxide dismutase (*SOD3*, downregulated), previously proposed as repressor molecule of skin inflammation (29). Cluster B is formed predominantly by a group of transcription factors (TF) (e.g. *PITX2*, a procollagen lysyl hydroxylase TF). Cluster C is represented by matrisome and matrisome-associated genes (http://matrisomeproject.mit.edu) (30), implicated in the stabilization, deposition and remodelling of the ECM (e.g. *TGFBI*, *FN1*, *TNC* and *POSTN*). Among the minor-clustered nodes, downregulation of *ALDH1A1* gene received our attention. This gene encodes an antioxidant enzyme related with UV-protection against oxidative stress (31) and is repressed by TGF-β (32). In our analysis, *ALDH1A1* is one of the most significant underexpressed genes in the three diseases.

Accepted Article

Validation of altered gene expression

Given the importance of the extracellular component – evidenced by enriched GO terms and KEGG pathways - we took advantage of the STRING PPI and chose several proteins of Cluster C for validation by western blot (Fig. 4). In this analysis we included additional patient and control samples not used for RNA-Seq (Table S1b). In accordance with transcriptomic data, fibulin-1, transglutaminase-2 (TG2) and ALDH1A1 were underexpressed in the diseases; while expression of tenascin-C, periostin and TGFBI were increased. In addition to the changes observed in these markers, we found high levels of α-sma in all genodermatoses fibroblasts confirming their activated phenotype (data not shown). Variability in protein expression levels in individual fibroblasts was observed, however, there was no evident pattern associated with body sites origin or age of donors. Abnormal expression of some of these proteins have been previously described in RDEB fibroblasts (33), but not the periostin overexpression. Thus, we decided to study their expression by immunofluorescence in available skin biopsy sections from RDEB and KS patients. The analysis showed a degree and pattern of overexpression similar to tenascin-C, used as positive control (Fig. 5).

Identification of serum periostin as a novel biomarker in RDEB

Increased levels of circulating periostin have been shown in several non-inherited fibrotic conditions including cancer (34,35). Considering the overexpression of periostin seen *in vitro* and *in situ*, we subsequently searched for periostin in available serum samples of RDEB patients and healthy donors. Consistently with the validation results, circulating periostin concentration were remarkably higher in RDEB patients (65,69ng/ml ± 14.75 SEM; n=16) compared to controls (3.72ng/ml ± 0.33 SEM; n=10) (p-value=0.0008; Fig. 6). This result suggests that periostin may represent a potential biomarker in RDEB.

Discussion

Here we conducted a global gene expression analysis of dermal fibroblasts - isolated from uninvolved skin areas of XPC, KS and RDEB patients - with the goal of elucidating overlapped pathomechanisms in these cancer-prone genodermatoses. Despite each disease's gene expression singularities, our study allowed to identify a common signature of 227

Accepted Article

transcripts and 4 KEGG pathways differentially expressed against healthy controls. Our different bioinformatic analyses revealed the presence of three major determinants of an activated fibroblast phenotype, namely: increased cell survival, altered TGF-ß signalling, and abnormal extracellular matrix remodelling (36,37). It is known that fibroblasts become activated when detect adverse cues from their surroundings - e.g. inflammation, mechanical trauma, TGF-ß, oxidative stress - and acquire a proliferative phenotype characterized by aberrant secretion of ECM molecules (38). Normally, activated fibroblasts return to their original state when the injury is resolved, through reprogramming or apoptosis (39). However, if the insult becomes chronic, fibroblasts become irreversibly active, just as it occurs in CAFs and fibrosis-associated fibroblasts (FAFs) (40).

The pathway inference analysis highlighted several nodes involving PI3K-Akt signalling activation, ultimately triggering anti-apoptotic and hyperproliferative stimuli via BCL2 effector protein. Earlier studies on RDEB have also shown that increased PI3K-Akt signalling mediates cell survival and cSCC development. Indeed, it was proposed as one pharmacological target to prevent disease progression (41). On the other hand, ontologies and categories referred to an altered activity of the cellular exterior, resulting in altered production of chemokine repertoire and abnormal expression of matrisome and matrisome-associated genes. The involvement of aberrantly expressed ECM proteins (e.g. tenascin-C, fibulin-1, transglutaminase-2, and TGFBI) was previously associated to loss of C7 (33,42). Overexpression of tenascin-C and TGF-β activation has also been shown in KS fibroblasts (14). To our knowledge, abnormal expression of periostin has not yet been reported in non-tumoral XPC, KS or RDEB fibroblasts, but was recently shown in RDEB-cSCC biopsies (43). Periostin and tenascin-C are induced by skin damage, promoting the activation of fibroblasts to repair the wound. Their overexpression has been linked to pathogenic roles in chronic inflammation, fibrosis and cancer (34,44,45). Different studies have shown that elevated levels of serum periostin are associated with progression and disease severity in pulmonary fibrosis (46), colorectal cancer (47,48) and systemic sclerosis (49). Our workflow from RNA-Seq to validation at protein level allowed us to disclose periostin as a possible systemic biomarker, at least in RDEB (due to sample availability). Currently, several experimental anti-fibrotic therapies are under investigation for this disease (28). Considering the paucity of available minimally invasive biomarkers to assess treatment efficacy, circulating periostin may be a useful molecule to consider. Further studies will be necessary to extend these results to XPC and KS.

Accepted Article

A general inferred notion from previous studies was that causal defects, such as loss of C7 or kindlin-1, could be accounted responsible for the abnormal ECM expression in RDEB and KS dermal fibroblasts (14,50,51). However, without excluding a triggering effect due to the primary deficiencies, our results challenge the view of a direct genetic cause-driven effect. Rather, they stand for the existence of a shared injury-responsive event able to transduce the primary defect into epigenetic changes, leading to an activated phenotype (Fig. 7). A likely candidate appears to be TGF-β since a large proportion of the common dysregulated genes (e.g. *TNC*, *POSTN, FN1, TGFBI*, and *ALDH1A1)* are modulated by this factor. Another possible candidate, already shown in XPC and KS (10,52–54), is oxidative stress which could be able, by itself or through their interaction with TGFβ, to trigger fibroblasts activation and ECM accumulation (55,56). In this context, downregulation of *ALDH1A1* and *SOD3* genes encoding for antioxidant enzymes could facilitate oxidative stress-induced damage. Similar expression changes in *ALDH1A1* were recently described as part of the myofibroblast-specific expression profile in mouse skin wounds (57). In fact, an *in-silico* comparison of our 186 dysregulated genes disclosed 41 overlapping genes included in the transcriptomic signature of mouse wound myofibroblasts. Overexpression of *POSTN* and *TNC*, stand out among these 41 genes (Fig. S2).

The examination of the exclusive transcriptional features of each disease may also offer interesting results, concerning the differential characteristics of each condition. However, these specific expression changes have not been the focus of this study and should be considered separately. All in all, the common genetic signature in fibroblasts of the three genodermatoses shares some similarities with that found in myofibroblasts (57), wound-activated fibroblasts and cutaneous CAFs (11). The common mechanisms of the three diseases would allow considering the use of symptom-relief therapies currently tested in RDEB, also in XPC and KS. In addition, the new elucidated molecular targets, such as those involved in a derangement of the oxidative state, could be subject to novel pharmacological approaches.

Accepted Article

References

1. DeStefano GM, Christiano AM. The Genetics of Human Skin Disease. Cold Spring Harb Perspect Med. 2014 Oct 1;4(10):a015172–a015172.

2. Fine J-D, Bruckner-Tuderman L, Eady RAJ, Bauer EA, Bauer JW, Has C, et al. Inherited epidermolysis bullosa: Updated recommendations on diagnosis and classification. J Am Acad Dermatol. 2014 Jun;70(6):1103–26.

3. Lotem M, Raben M, Zeltser R, Landau M, Sela M, Wygoda M, et al. Kindler syndrome complicated by squamous cell carcinoma of the hard palate: successful treatment with high-dose radiation therapy and granulocyte-macrophage colony-stimulating factor. Br J Dermatol. 2001 Jun;144(6):1284–6.

4. Jobard F, Bouadjar B, Caux F, Hadj-Rabia S, Has C, Matsuda F, et al. Identification of mutations in a new gene encoding a FERM family protein with a pleckstrin homology domain in Kindler syndrome. Hum Mol Genet. 2003 Apr 15;12(8):925–35.

5. Siegel DH, Ashton GHS, Penagos HG, Lee J V., Feiler HS, Wilhelmsen KC, et al. Loss of Kindlin-1, a Human Homolog of the Caenorhabditis elegans Actin–Extracellular-Matrix Linker Protein UNC-112, Causes Kindler Syndrome. Am J Hum Genet. 2003 Jul;73(1):174–87.

6. Kraemer KH, Lee MM, Scotto J. Xeroderma pigmentosum. Cutaneous, ocular, and neurologic abnormalities in 830 published cases. Arch Dermatol. 1987 Feb;123(2):241–50.

7. DiGiovanna JJ, Kraemer KH. Shining a Light on Xeroderma Pigmentosum. J Invest Dermatol. 2012 Mar;132(3):785–96.

8. Rezvani HR, Kim AL, Rossignol R, Ali N, Daly M, Mahfouf W, et al. XPC silencing in normal human keratinocytes triggers metabolic alterations that drive the formation of squamous cell carcinomas. J Clin Invest. 2011 Jan 4;121(1):195–211.

9. Breitenbach JS, Rinnerthaler M, Trost A, Weber M, Klausegger A, Gruber C, et al. Transcriptome and ultrastructural changes in dystrophic Epidermolysis bullosa resemble skin aging. Aging (Albany NY). 2015;7(6):389–411.

10. Maier K, He Y, Wölfle U, Esser PR, Brummer T, Schempp C, et al. UV-B-induced cutaneous inflammation and prospects for antioxidant treatment in Kindler syndrome. Hum Mol Genet. 2016;25(24):5339–52.

11. Ng Y-Z, Pourreyron C, Salas-Alanis JC, Dayal JHS, Cepeda-Valdes R, Yan W, et al. Fibroblast-Derived Dermal Matrix Drives Development of Aggressive Cutaneous Squamous Cell Carcinoma in Patients with Recessive Dystrophic Epidermolysis Bullosa. Cancer Res. 2012;72(14):3522–34.

12. Bernerd F, Asselineau D, Vioux C, Chevallier-Lagente O, Bouadjar B, Sarasin A, et al. Clues to epidermal cancer proneness revealed by reconstruction of DNA repair-deficient xeroderma pigmentosum skin in vitro. Proc Natl Acad Sci U S A. 2001 Jul 3;98(14):7817–22.

13. Fréchet M, Warrick E, Vioux C, Chevallier O, Spatz A, Benhamou S, et al.

Accepted Article

Overexpression of matrix metalloproteinase 1 in dermal fibroblasts from DNA repair-deficient/cancer-prone xeroderma pigmentosum group C patients. Oncogene. 2008 Sep 12;27(39):5223–32.

14. Heinemann A, He Y, Zimina E, Boerries M, Busch H, Chmel N, et al. Induction of phenotype modifying cytokines by FERMT1 mutations. Hum Mutat. 2011 Apr;32(4):397–406.

15. Zamarrón A, García M, Del Río M, Larcher F, Juarranz Á. Effects of photodynamic therapy on dermal fibroblasts from xeroderma pigmentosum and Gorlin-Goltz syndrome patients. Oncotarget. 2017 Sep 29;8(44):77385–99.

16. Meana A, Iglesias J, Del Rio M, Larcher F, Madrigal B, Fresno M., et al. Large surface of cultured human epithelium obtained on a dermal matrix based on live fibroblast-containing fibrin gels. Burns. 1998 Nov 1;24(7):621–30.

17. Robinson MD, Oshlack A. A scaling normalization method for differential expression analysis of RNA-seq data. Genome Biol. 2010;11(3):R25.

18. Johnson WE, Li C, Rabinovic A. Adjusting batch effects in microarray expression data using empirical Bayes methods. Biostatistics. 2007 Jan 1;8(1):118–27.

19. Robinson MD, McCarthy DJ, Smyth GK. edgeR: a Bioconductor package for differential expression analysis of digital gene expression data. Bioinformatics. 2010 Jan 1;26(1):139–40.

20. Benjamini Y, Hochberg Y. Controlling the False Discovery Rate: A Practical and Powerful Approach to Multiple Testing. Vol. 57, Journal of the Royal Statistical Society. Series B (Methodological). WileyRoyal Statistical Society; 1995. p. 289–300.

21. Alonso R, Salavert F, Garcia-Garcia F, Carbonell-Caballero J, Bleda M, Garcia-Alonso L, et al. Babelomics 5.0: functional interpretation for new generations of genomic data. Nucleic Acids Res. 2015 Jul 1;43(W1):W117-21.

22. Huang DW, Sherman BT, Lempicki RA. Bioinformatics enrichment tools: paths toward the comprehensive functional analysis of large gene lists. Nucleic Acids Res. 2009 Jan;37(1):1–13.

23. Hidalgo MR, Cubuk C, Amadoz A, Salavert F, Carbonell-Caballero J, Dopazo J. High throughput estimation of functional cell activities reveals disease mechanisms and predicts relevant clinical outcomes. Oncotarget. 2017 Jan 17;8(3):5160–78.

24. Szklarczyk D, Franceschini A, Wyder S, Forslund K, Heller D, Huerta-Cepas J, et al. STRING v10: protein–protein interaction networks, integrated over the tree of life. Nucleic Acids Res. 2015 Jan 28;43(D1):D447–52.

25. Escámez MJ, García M, Cuadrado-Corrales N, Llames SG, Charlesworth A, De Luca N, et al. The first *COL7A1* mutation survey in a large Spanish dystrophic epidermolysis bullosa cohort: c.6527insC disclosed as an unusually recurrent mutation. Br J Dermatol. 2010 Apr;163(1):155–61.

26. Ashburner M, Ball CA, Blake JA, Botstein D, Butler H, Cherry JM, et al. Gene Ontology: tool for the unification of biology. Nat Genet. 2000 May;25(1):25–9.

Accepted Article

27. Kanehisa M, Goto S, Sato Y, Furumichi M, Tanabe M. KEGG for integration and interpretation of large-scale molecular data sets. Nucleic Acids Res. 2012 Jan 1;40(D1):D109–14.

28. Nyström A, Thriene K, Mittapalli V, Kern JS, Kiritsi D, Dengjel J, et al. Losartan ameliorates dystrophic epidermolysis bullosa and uncovers new disease mechanisms. EMBO Mol Med. 2015;7(9):1211–28.

29. Kwon M-J, Kim B, Lee YS, Kim T-Y. Role of superoxide dismutase 3 in skin inflammation. J Dermatol Sci. 2012 Aug;67(2):81–7.

30. Naba A, Clauser KR, Ding H, Whittaker CA, Carr SA, Hynes RO. The extracellular matrix: Tools and insights for the "omics" era. Matrix Biol. 2016 Jan;49:10–24.

31. Lassen N, Bateman JB, Estey T, Kuszak JR, Nees DW, Piatigorsky J, et al. Multiple and Additive Functions of ALDH3A1 and ALDH1A1. J Biol Chem. 2007 Aug 31;282(35):25668–76.

32. Hoshino Y, Nishida J, Katsuno Y, Koinuma D, Aoki T, Kokudo N, et al. Smad4 Decreases the Population of Pancreatic Cancer–Initiating Cells through Transcriptional Repression of ALDH1A1. Am J Pathol. 2015 May;185(5):1457–70.

33. Küttner V, MacK C, Rigbolt KTG, Kern JS, Schilling O, Busch H, et al. Global remodelling of cellular microenvironment due to loss of collagen VII. Mol Syst Biol. 2013;9(657):1–14.

34. Yamaguchi Y. Periostin in Skin Tissue Skin-Related Diseases. Allergol Int. 2014;63(2):161–70.

35. González-González L, Alonso J. Periostin: A Matricellular Protein With Multiple Functions in Cancer Development and Progression. Front Oncol. 2018 Jun 12;8:225.

36. Tomasek JJ, Gabbiani G, Hinz B, Chaponnier C, Brown RA. Myofibroblasts and mechano-regulation of connective tissue remodelling. Nat Rev Mol Cell Biol. 2002 May 1;3(5):349–63.

37. Parsonage G, Filer AD, Haworth O, Nash GB, Rainger GE, Salmon M, et al. A stromal address code defined by fibroblasts. Trends Immunol. 2005 Mar;26(3):150–6.

38. Vong S, Kalluri R. The Role of Stromal Myofibroblast and Extracellular Matrix in Tumor Angiogenesis. Genes Cancer. 2011 Dec 1;2(12):1139–45.

39. Micallef L, Vedrenne N, Billet F, Coulomb B, Darby IA, Desmoulière A. The myofibroblast, multiple origins for major roles in normal and pathological tissue repair. Fibrogenesis Tissue Repair. 2012;5(Suppl 1):S5.

40. Kalluri R. The biology and function of fibroblasts in cancer. Nat Rev Cancer. 2016;16(9):582–98.

41. Mittapalli VR, Madl J, Lï¿½ffek S, Kiritsi D, Kern JS, Rï¿½mer W, et al. Injury-driven stiffening of the dermis expedites skin carcinoma progression. Cancer Res. 2016;76(4):940–51.

42. Küttner V, Mack C, Gretzmeier C, Bruckner-Tuderman L, Dengjel J. Loss of collagen

Accepted Article

VII is associated with reduced transglutaminase 2 abundance and activity. J Invest Dermatol. 2014;134(9):2381–9.

43. Föll MC, Fahrner M, Gretzmeier C, Thoma K, Biniossek ML, Kiritsi D, et al. Identification of tissue damage, extracellular matrix remodeling and bacterial challenge as common mechanisms associated with high-risk cutaneous squamous cell carcinomas. Matrix Biol. 2018;66(2018):1–21.

44. Midwood KS, Chiquet M, Tucker RP, Orend G. Tenascin-C at a glance. J Cell Sci. 2016 Dec 1;129(23):4321–7.

45. Yang L, Serada S, Fujimoto M, Terao M, Kotobuki Y, Kitaba S, et al. Periostin Facilitates Skin Sclerosis via PI3K/Akt Dependent Mechanism in a Mouse Model of Scleroderma. Rossini A, editor. PLoS One. 2012 Jul 24;7(7):e41994.

46. Naik PK, Bozyk PD, Bentley JK, Popova AP, Birch CM, Wilke CA, et al. Periostin promotes fibrosis and predicts progression in patients with idiopathic pulmonary fibrosis. Am J Physiol Lung Cell Mol Physiol. 2012 Dec 15;303(12):L1046-56.

47. Ben Q-W, Zhao Z, Ge S-F, Zhou J, Yuan F, Yuan Y-Z. Circulating levels of periostin may help identify patients with more aggressive colorectal cancer. Int J Oncol. 2009 Mar;34(3):821–8.

48. Dong D, Zhang L, Jia L, Ji W, Wang Z, Ren L, et al. Identification of Serum Periostin as a Potential Diagnostic and Prognostic Marker for Colorectal Cancer. Clin Lab. 2018 Jun 1;64(6):973–81.

49. Yamaguchi Y, Ono J, Masuoka M, Ohta S, Izuhara K, Ikezawa Z, et al. Serum periostin levels are correlated with progressive skin sclerosis in patients with systemic sclerosis. Br J Dermatol. 2013 Apr;168(4):717–25.

50. Cianfarani F, Zambruno G, Castiglia D, Odorisio T. Pathomechanisms of Altered Wound Healing in Recessive Dystrophic Epidermolysis Bullosa. Am J Pathol. 2017;187(7):1445–53.

51. Bruckner-Tuderman L, Has C. Disorders of the cutaneous basement membrane zone—The paradigm of epidermolysis bullosa. Matrix Biol. 2014 Jan;33:29–34.

52. Zapatero-Solana E, García-Giménez JL, Guerrero-Aspizua S, García M, Toll A, Baselga E, et al. Oxidative stress and mitochondrial dysfunction in Kindler syndrome. Orphanet J Rare Dis. 2014 Dec 21;9(1):211.

53. Emmert H, Patel H, Brunton VG. Kindlin-1 protects cells from oxidative damage through activation of ERK signalling. Free Radic Biol Med. 2017;108(May):896–903.

54. Hosseini M, Ezzedine K, Taieb A, Rezvani HR. Oxidative and Energy Metabolism as Potential Clues for Clinical Heterogeneity in Nucleotide Excision Repair Disorders. J Invest Dermatol. 2015 Feb;135(2):341–51.

55. Liu RM, Desai LP. Reciprocal regulation of TGF-β and reactive oxygen species: A perverse cycle for fibrosis. Redox Biol. 2015;6:565–77.

56. Richter K, Kietzmann T. Reactive oxygen species and fibrosis: further evidence of a significant liaison. Cell Tissue Res. 2016 Sep 27;365(3):591–605.

57. Bergmeier V, Etich J, Pitzler L, Frie C, Koch M, Fischer M, et al. Identification of a myofibroblast-specific expression signature in skin wounds. Matrix Biol. 2018;65:59–74.

Accepted Article

Accepted Article

TABLES

Table 1. Number of genes differentially expressed in each genodermatosis versus healthy controls.

Differentially expressed genes			
Comparison	Under-expressed*	Over-expressed*	Total DE
RDEB vs Ctrl	516	327	843
KS vs Ctrl	196	180	376
XPC vs Ctrl	523	509	1032

* Under- or over-expressed genes in the diseases.

Accepted Article

FIGURES LEGENDS

Fig. 1. Differential gene expression profile. (a) PCA-plot represents the global distribution of each sequenced sample, after data processing and normalization. Disease samples tend to group together and distantly from the controls. (b) An overlapping set of 227 transcripts, were commonly dysregulated in all the diseases (Venn diagram). (c) Heatmap of the normalized expression of the 227 transcripts (detailed in Table S3d) is shown (red: upregulated, green: downregulated in the disease). (d) Linear regression of fold changes of the 227 transcripts (blue dots) shows an impressive positive correlation (R^2=0.895). Axes indicate fold change values (logarithmic scale).

Fig. 2. Enrichment analysis of differentially expressed genes. Within the specific alterations of each disease, enriched GO terms highlight common abnormalities in the three genodermatoses with respect to cell periphery, extracellular matrix and activity of transcription factors. KEGG pathways reveal enriched categories related with cancer, PI3K-Akt and chemokine signalling. The highest ranked categories in each disease are shown according to the p-value and percentage of genes.

Fig. 3. Protein-protein interaction network of the common dysregulated genes. The three largest connected components, labelled as "Cluster A, B and C", represent a cluster of highly-connected, biologically related proteins. Node colour is graded according to the average fold change (red: upregulated, green: downregulated in the disease). Edge width is proportional to STRING interaction score, which represents the confidence for that interaction. Groups of potentially interactive proteins with fewer nodes are shown below the main clusters. Proteins without interactions are not shown. The average node degree is 0.387 and the average local clustering coefficient is 0.158.

Accepted Article

Fig. 4. Western blot validation of relevant genes. Immunoblot analysis of fibroblast cell-lysates confirm the high expression of tenascin-C, periostin and TGFBI, together with an underexpression of TG2, ALDH1A1 and fibulin-1 in samples from RDEB, XPC and KS patients. GAPDH was used as loading control. Samples not included in the RNA-Seq are indicated by an asterisk (*).

Fig. 5. Immunofluorescence *in situ* validation of tenascin-C and periostin. Skin biopsies sections from RDEB, KS and healthy controls were stained for (a) tenascin-C and (b) periostin. Quantitation of fluorescence intensity was measured on five non-overlapping microscopic fields per sample (ImageJ) and represented as mean staining intensity/area value +/- SD. The data were analysed by Students t-test *$p<0.05$; ** $p<0.01$.

Fig. 6. Circulating periostin levels in RDEB patients. Serum periostin concentration was significantly higher in RDEB patients (65.69ng/ml ± 14.75 SEM; n=16) compared to donor controls (3.72ng/ml ± 0.33 SEM; n=10). Two independent experiments were performed for each patient sample and controls. ***p-value=0.0008.

Fig.7. Model of the common pathomechanism suggested for RDEB, XPC and KS. Genodermatoses fibroblasts respond similarly to tissue injury and inflammation. These persistent stimuli may converge into the activation of TGF-β signalling and oxidative imbalance, which lead the overexpression of ECM proteins (e.g. TNC, POSTN and FN1) and the reduction of antioxidant enzymes (e.g. ALDH1A1 and SOD3). Reciprocal regulation between TGF-β and ROS allows the acquisition of an activated and synthetic fibroblast phenotype and may promote the disease progression.

Accepted Article

Supporting information

Fig. S1. Pathway activity analysis. (a) Venn diagram, derived from the *Hipathia* analysis, reveals an overlapping set of 42 signalling circuits common to the three genodermatoses (detailed in Table S5). (b) Representation of the BCL2-mediated apoptosis inhibition circuit. The increased activity of BCL2 (final effector of the pathway) is initiated mainly by the overexpression of *HRAS* and *RAC1*. This leads to the activation of PI3K-Akt signalling which, together with the overexpression of *YWHAQ*, inactivates the action of BAD (a repressor of BCL2), thus preventing cell apoptosis.

Fig. S2. Venn Diagram of dysregulated genes in myofibroblasts and genodermatoses fibroblasts. The comparison revealed an overlap of 41 altered genes, including *POSTN*, *TNC* and *ALDH1A1*.

Table S1. Patient information. Age, sex and gene/protein mutation of all patient and control samples used in (a) RNA-Seq and (b) validation analysis.

Table S2. Normalized RNA-Seq counts for all genes and all samples.

Table S3. Differentially expressed genes (FDR<0.05). (a) RDEB vs Ctrl; (b) XPC vs Ctrl; (c) KS vs Ctrl.

Table S4. Gene Ontology and KEGG enrichment analysis. GO terms (cellular components and molecular functions) and KEGG enriched pathways (p-value <0.1) obtained from genes differentially expressed in (a) RDEB vs Ctrl; (b) KS vs Ctrl; (c) XPC vs Ctrl.

Table S5. Pathway activity analysis. Signalling enriched *Hipathia* circuits (adjusted p-value<0.05) obtained from genes differentially expressed in (a) RDEB vs Ctrl; (b) KS vs Ctrl; (c) XPC vs Ctrl. In orange, circuits altered in the three diseases.

Accepted Article

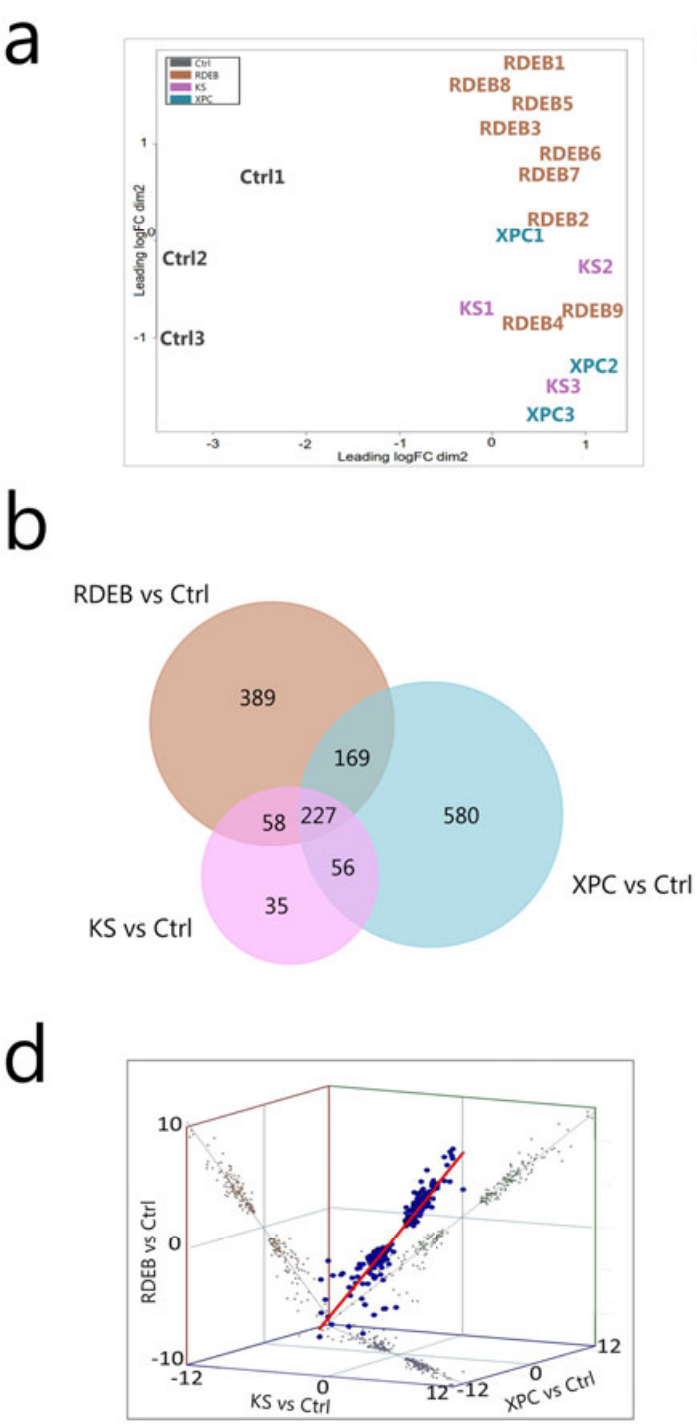

Fig. 1

Accepted Article

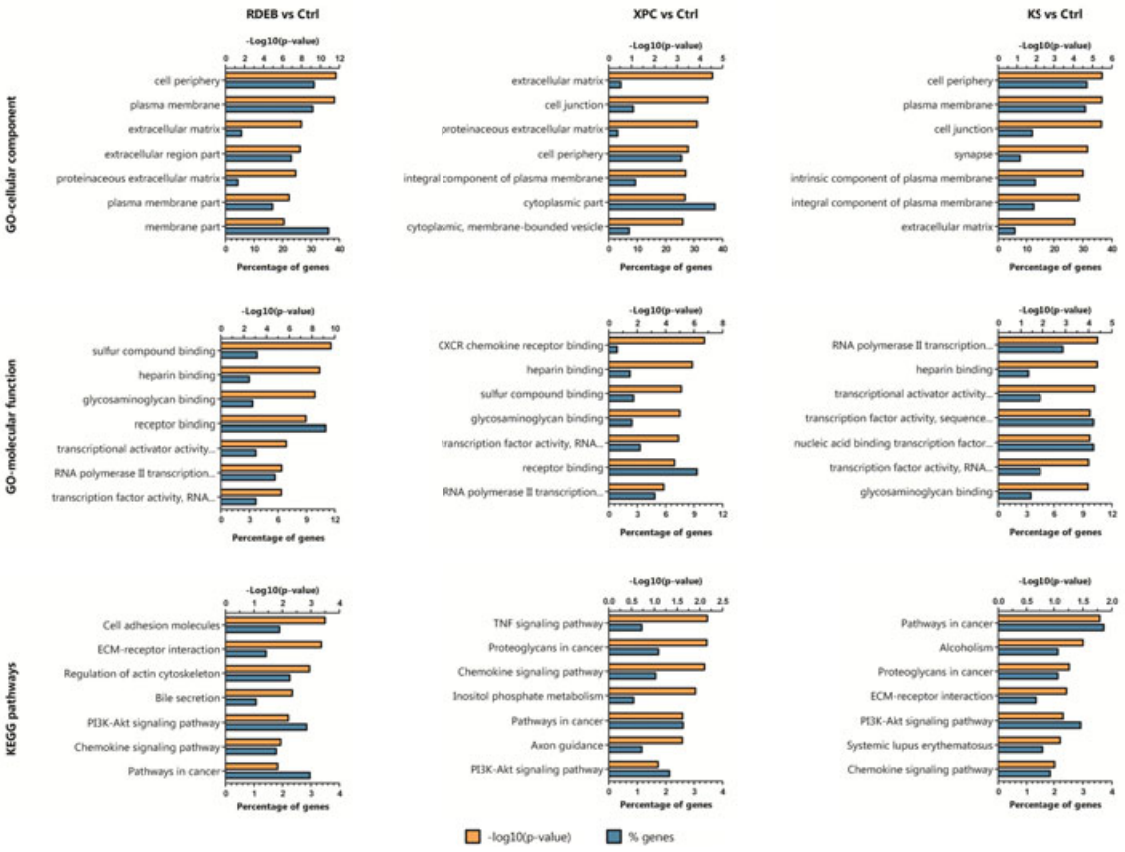

Accepted Article

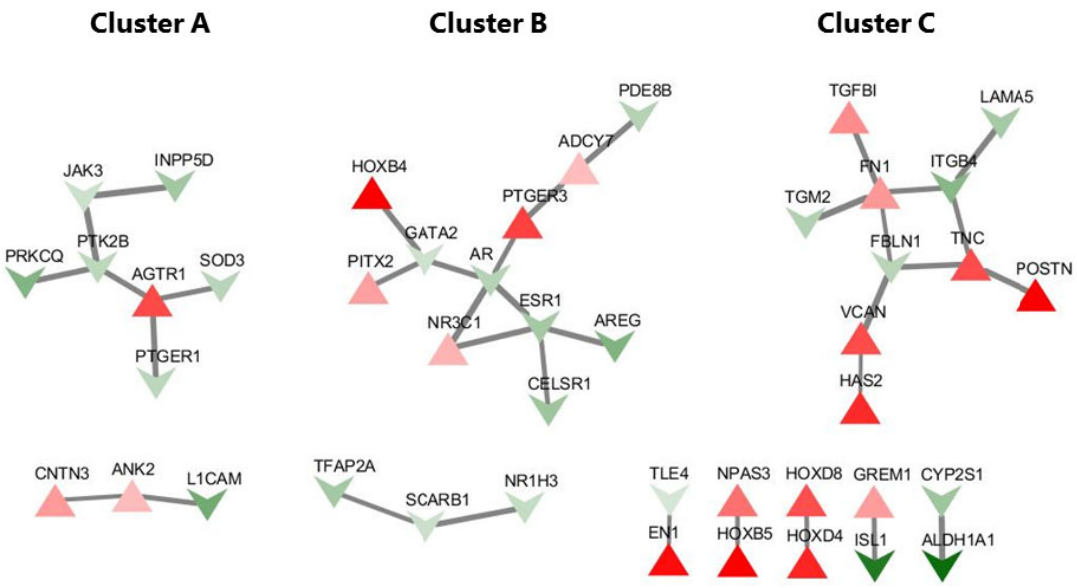

Fig. 3

Accepted Article

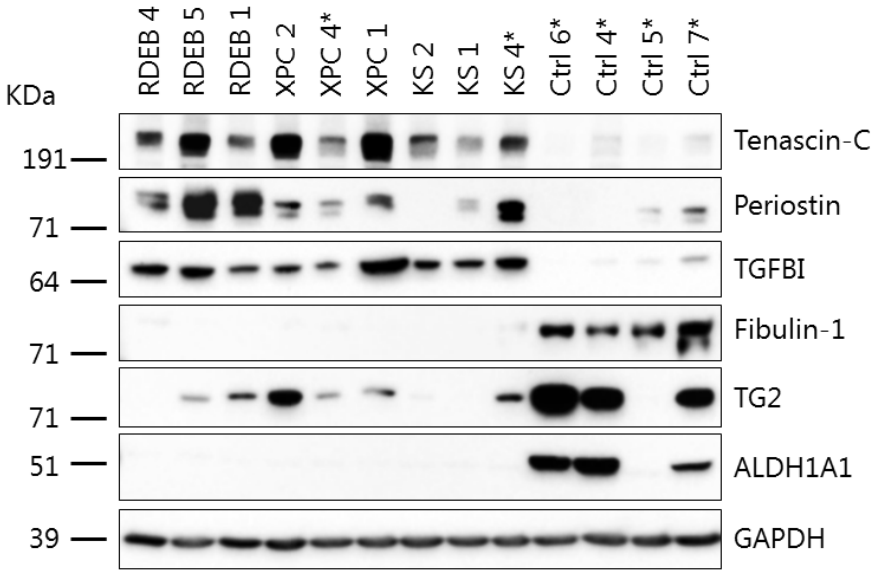

Fig. 4

Accepted Article

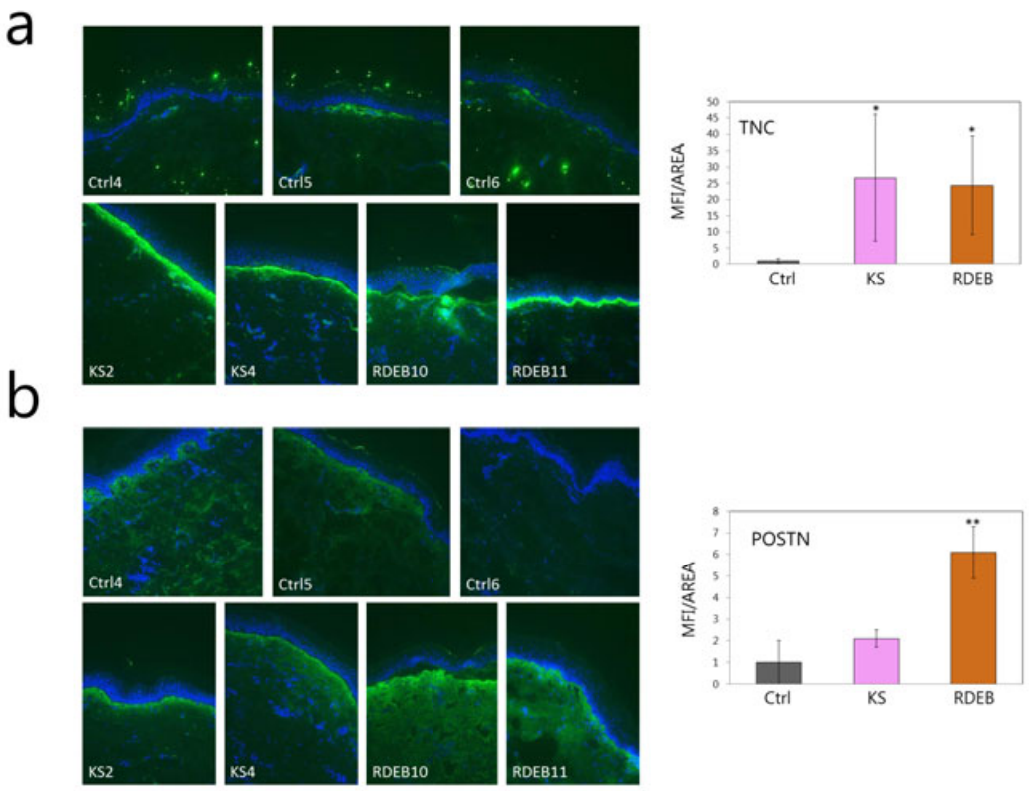

Fig. 5

Accepted Article

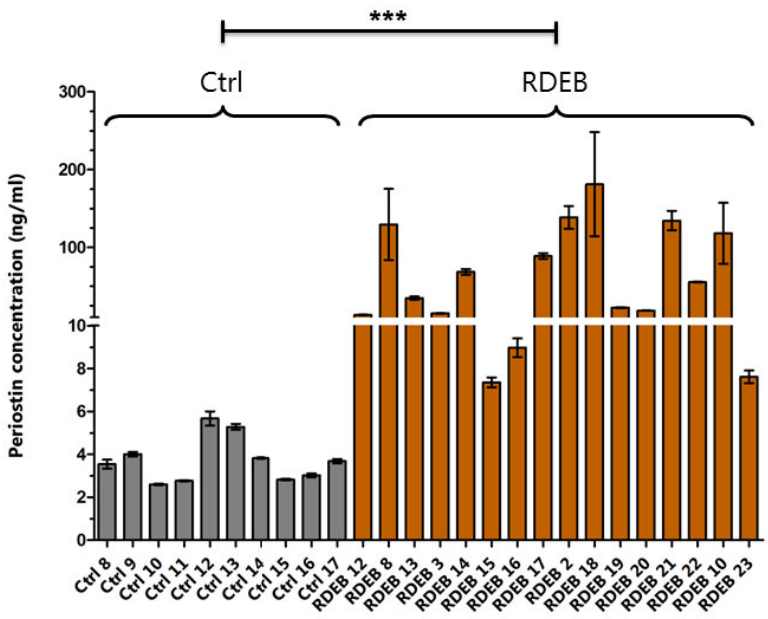

Fig. 6

Accepted Article